Development of a Real Time "Front End" Time-Domain Calibration System for the Advanced LIGO Detectors

Craig Cahillane

Caltech LIGO SURF 2013

Mentors: Alan Weinstein and Jameson Rollins

August 2, 2013

Abstract

The Advanced LIGO gravitational wave detectors are currently under construction along with new, more precise calibration control systems. Our goal is to understand the Advanced LIGO detectors response to incident gravitational waves. During detector operation, parameters characterizing the detector can change in real time, altering the detectors response to gravitational waves. These changes in the detector response must be tracked and taken into consideration when calibrating gravitational wave strain. We propose instituting a real time front-end time-domain calibration system in order to better track the changes of the detector response during science runs. Development of such a calibration system is underway at the Caltech 40m interferometer.

1 Introduction

The Laser Interferometer Gravitational-Wave Observatory (LIGO) is a network of three detectors built to detect local perturbations in the space-time metric known as strain from astrophysical sources. The anticipated size of these perturbations is 10^{-23}m, less than one ten-thousandth of the diameter of a proton. [4] Extreme care is taken to shield the detectors from noise, but not all noise can be prevented. This means true gravitational wave strain is difficult to discern due to low signal-to-noise ratio. Calibration allows us to measure how the detector will respond to an incident gravitational wave strain.

1.1 Advanced LIGO Detectors

At the heart of the Advanced LIGO detectors resides a dual-recycled Fabry-Perot Michelson interferometer. A Michelson interferometer consists of a laser beam fired into a beam splitter, allowing half of the laser light straight through
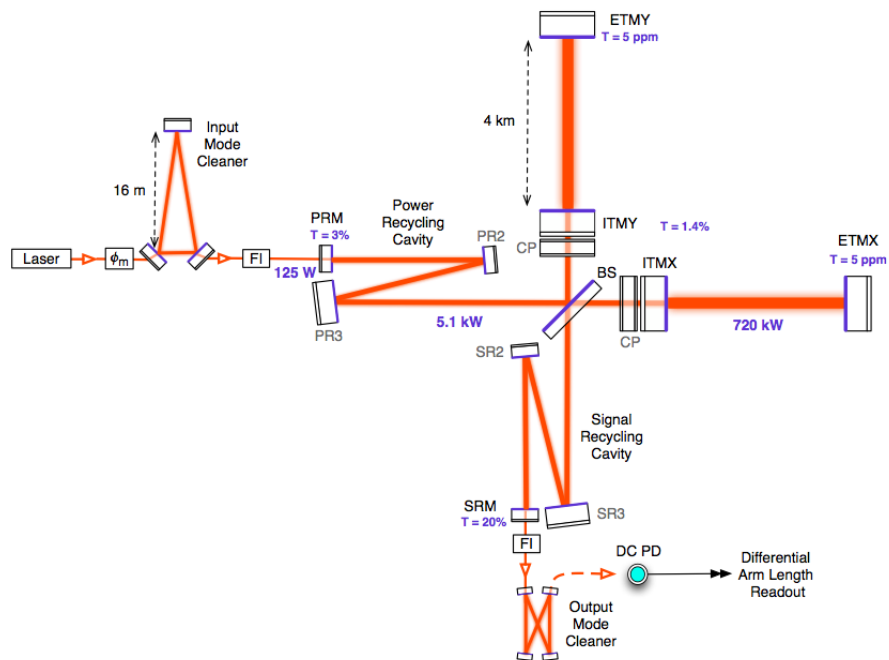
Figure 1: Advanced LIGO Michelson Interferometer diagram. The ETM and ITM form the Fabry Perot cavities, while the three PRM and two ITM form the power recycling cavity. If both arms are an integral number of wavelengths of laser light, then all light in the Signal Recycling AS port destructively interferes and the interferometer is said to be "on resonance". Image from [4]

and deflecting the other half 90 degrees. The light in the interferometer is phase modulated to produce Radio Frequency (RF) sidebands at $\omega_m \approx 2\pi \times 25$ MHz. The original frequency of light, called the carrier frequency, is tuned for constructive interference within the Fabry-Perot cavities. The sideband frequencies are not tuned to resonate in the Fabry-Perot cavities, and instead reside largely in the Power Recycling Cavity and Signal Recycling Cavity to aid in signal extraction.

The carrier light travels in perpendicular arms of the same length until it hits a reflecting mirror. This reflected light carries back with it a phase difference based on the microscopic difference in length the light has traveled. This difference in the arm lengths is known as the differential arm length, or DARM. When the DARM is zero, there is no phase difference in the light, and by destructive interference no carrier band light enters the photodiode at the Antisymmetric (AS) port. When there exists a phase difference in the light, we can detect the optics' movement by detecting carrier band light beating with the sideband light frequencies in the AS port. [5] This change in the DARM length includes both noise and astrophysical strain signal.

1.2   Frequency Domain Calibration

A feedback loop keeps the interferometer in its resonance condition. Resonance condition is when the distance between the mirrors of the interferometer is an integer value of the wavelength of laser light in the interferometer. When this occurs, the reflected light constructively interferes in the power recycling cavity and destructively interferes in the signal recycling cavity, or the AS port. This resonance condition is maintained by a servo actuator that responds to a digital error signal $e_D(f)$. $e_D(f)$ is proportional to the DARM length change $\Delta L_{ext}(f)$ and feedback actuation length $\Delta L_A(f)$. The error signal $e_D(f)$ is the result of the digitization of the analog signal registered by the interferometer, and, most important, it has a linear relationship when in resonance condition:

$$\Delta L_{ext} = R_L(f)e_D(f) \tag{1}$$

where $R_L(f)$ is the response function. In the long wavelength approximation, ΔL_{ext} is linearly related to gravitational wave strain $h(f)$:

$$h(f) = \frac{\Delta L_{ext}}{L} \tag{2}$$

where L is the measured length of the arm cavities. Finding this linear response function is a process known as frequency-domain calibration. [1] [3]

1.3   Feedback Control Loop

We want to preserve the linear relation between $e_D(f)$ and gravitational strain $h(f)$, so feedback control loops are used to keep DARM close to zero. In this linear domain we must measure the response function $R_L(f, t)$ accurately to get an accurate strain signal.
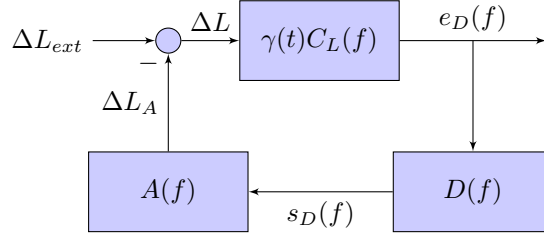
Figure 2: Visualization of the Feedback Control System Loop. The interferometer senses a change in the DARM length ΔL_{ext} and receives feedback input ΔL_A, producing a digital error signal $e_D(f)$. The digital filters $D(f)$ produce a digital control signal $s_D(f)$. Finally, the actuation function $A(f)$ determines the motion necessary to keep the interferometer in its resonance condiction, sending a new actuation ΔL_A.

The response function $R_L(f, t)$ depends on the sensing function $C_L(f)$, digital filters $D(f)$, and actuation function $A(f)$ in the following relationship:

$$R_L(f, t) \equiv \frac{1 + \gamma(t)G_L(f)}{\gamma(t)C_L(f)} \tag{3}$$

where $\gamma(t)$ is the slow time dependence of the sensing function's $C_L(f)$ and $G_L(f) = C_L(f)D(f)A(f)$ is the open loop gain.

$R_L(f)$ is important because the convolution kernel $R_L(t - t')$ can be reproduced from it, and this convolution kernel is used to reconstruct the gravitational strain $h(t)$ in the equation:

$$h(t) = \frac{1}{L} \int R_L(t - t')e_D(t')dt' \tag{4}$$

The open loop gain $G_L(f)$ is separated into three components: $G_L(f) = C_L(f)D(f)A(f)$. Each of these three components is crucial to the overall response function of the detector. $C_L(f)$, the sensing function, captures the analog $\Delta L_{ext}(f)$ and converts it into a digital signal $e_D(f)$. A photodiode detects how much carrier light reaches the AS port, which determines $\Delta_{ext}L(f)$, then runs this analog signal through the sensing function $C_L(f)$, here approximated to a single cavity pole transfer function:

$$C_L(f) \approx \frac{1}{1 + i\frac{f}{f_c}} \tag{5}$$

where f_c is the cavity pole frequency and i is the imaginary unit. [4] [1] $D(f)$, the digital filter, converts $e_D(f)$ into a digital control signal $s_D(f)$ to be sent back to the detector mirror. $A(f)$, the actuation function, converts $s_D(f)$ into an analog signal that physically moves the mirrors. In Initial LIGO, the mirrors
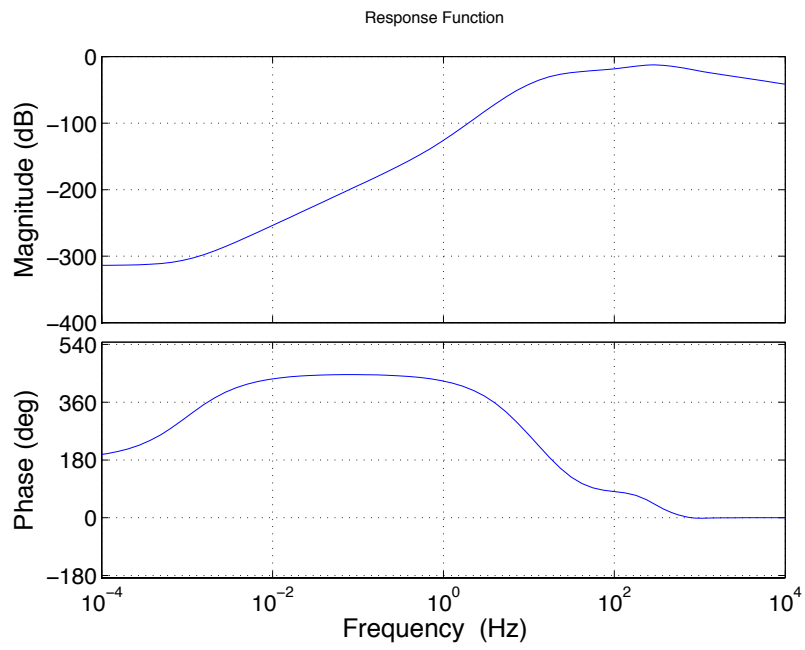
Figure 3: Response Function Bode Plot. The response function $R_L(f)$ plotted with respect to frequency. In the linear resonance condition, we multiply this function by $e_D(f)$ to get $h(f)$, the GW strain in the frequency domain. This plot created with parameters from Hanford interferometer H1 in S5. [1]

that reflect the laser light are pendulums, and the pendulums' natural frequency response yields a good approximation for the complete actuation function:

$$A(f) \approx \frac{1}{f_p^2 - f^2 + i\frac{f_p f}{Q}} \qquad (6)$$

where f_p is the natural frequency of the pendulum and Q is the quality damping factor. [4] [1]

From Figure 3, we see two different signals can be used to reconstruct ΔL_{ext}: the error signal $e_D(f)$ and control signal $s_D(f)$. From Equations (1) and (3), ignoring the factor $\gamma(t)$, we get

$$\Delta L_{ext} = \frac{1+G}{C_L} e_D \qquad (7)$$

$$\Delta L_{ext} = A\frac{1+G}{G} s_D \qquad (8)$$

The properties of the open loop gain G at certain frequencies make the use of both of these signals essential. As frequency f goes to zero, the open loop gain G goes to infinity, causing Equation (7) to blow up at low frequencies. Alternatively, as frequency f goes to high frequency G must goes to zero to keep the loop stable. This causes Equation (8) to blow up. However, we can combine the two, using the control signal at low frequencies and the error signal at high frequencies:

$$\Delta L = \Delta L_{ext} - \Delta L_A$$
$$\Delta L_{ext} = \Delta L + \Delta L_A$$

From Figure 2 we can see that $\Delta L = \frac{e_D}{C_L}$ and $\Delta L_A = s_D A$, giving

$$\Delta L_{ext} = \frac{e_D}{C_L} + s_D A \qquad (9)$$

From Equation (9) we see that this method of strain reconstruction completely avoids the digital filters D, allowing for changes to the filters to be made in real time with no repercussions in the calibration control system.

1.4   Time Domain Calibration

However, there are ways to calculate $h(t)$ directly from the frequency domain response. For Advanced LIGO we want to track the system changes in real time more closely. In order to do this we want to implement a time-domain calibration system at the front end, so changes in the detector response are immediately found and accounted for. We must first check if the time-domain system can give us a better calibration and quantify the errors in its calculation. If the time-domain system proves to be useful, it can potentially reduce our uncertainty in the gravitational wave strain $h(t)$. [2]
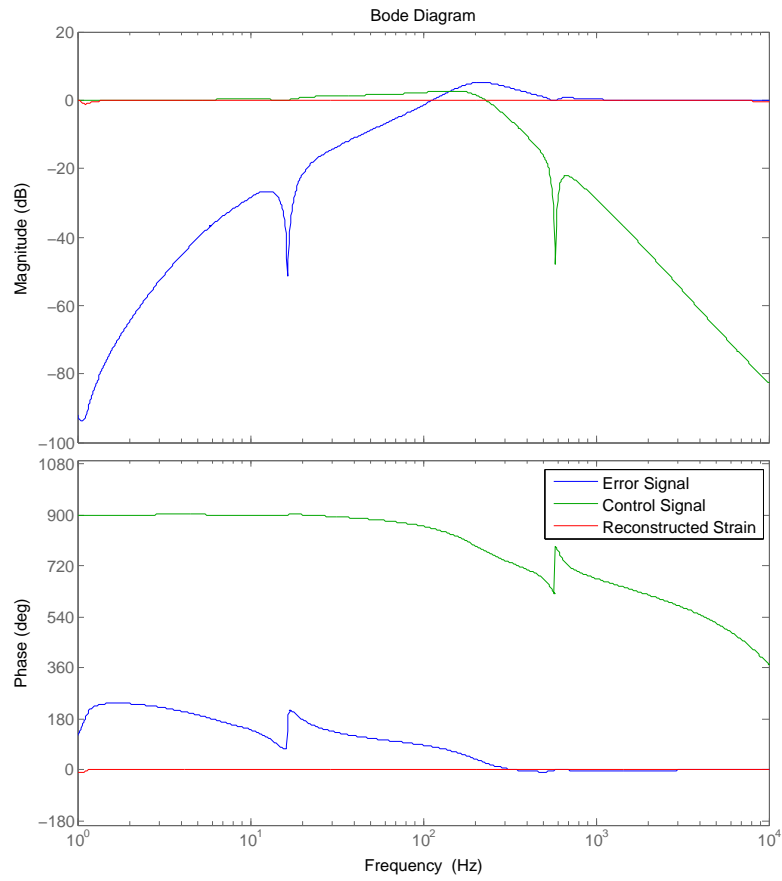
Figure 4: Reconstruction of Strain in the Frequency Domain from the Error and Control Signals. The strain magnitude levels at zero decibles, giving near perfect signal reconstruction capabilities from this method. [6]
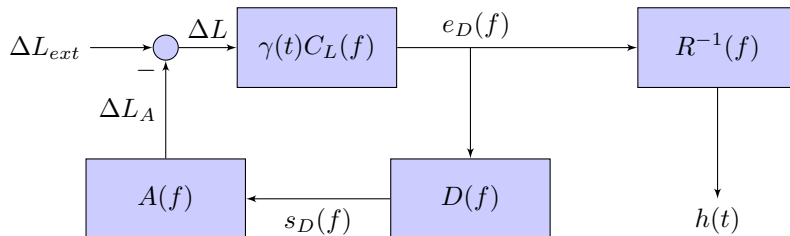
7

Figure 5: Reimagined 40m Interferometer Feedback Control System. The inverse response function $R^{-1}(f)$ immediately takes the error signal $e_D(f)$ and converts it to the strain signal $h(t)$ sensed by the interferometer in the time domain. This occurs before on the "Front End", before the digital filters $D(f)$ alter the signal.

In the case of an interferometer, we want to convert counts into meters representing the DARM displacement. For a time domain calibrator, we will run the inverse of the linear response function $R^{-1}(f)$ on the error signal $e_D(f)$, producing the strain signal $h(t)$. But the response function is changing in real time, so we must measure how $R(f)$ and $R^{-1}(f)$ are changing and adjust them accordingly. To do this in real time, calibration lines are input into the interferometer at specified frequencies of known magnitude and phase. The calibrator will demodulate at the calibration line frequencies and analyze how the signal has changed due to changes in the response function. From this information, we should be able to construct the ever-important inverse response function $R^{-1}(f)$ as it changes in time.

2   Objectives

Instead of performing "downstream" calibrations, we hope to implement the calibration system within the digital control system, and thereby track the time changes of the component response functions more effectively. The calibration system will be built as a component of the control system at the Caltech 40m interferometer. By the end of the project, we hope to use the Caltech 40m interferometer to generate data, use the new subsystem to calibrate it, and compare the calibrated signal to what we expect the measurement to be. To calibrate the detectors, calibration lines are injected into the system at known frequencies. The calibration lines' response to the control loop are tracked, giving an idea of how noise and GW strain respond to the control loop. Using this new method of calibration, we aim to accurately track the real-time changes in the detector response function, thus generating a faster, more reliable way of calculating gravitational wave strain.

3 Approach

The calibration code will be written in MATLAB and Simulink, using tools for linear time domain filtering to sort signal from noise. We will start calibrating the signals from the more simple interferometer configurations and quantifying the errors involved with our new method. Next, we will move on to the more complex interferometer signals to get a complete picture of the DARM interferometer signals. Finally, we hope to piece together all of the parts into a actual real-time control system for the interferometer.

4 Project Schedule

For the first two weeks, I will become intimately acquainted with the Caltech 40m interferometer different function modes while understanding a traditional frequency model in MATLAB. In the next two weeks, we will finish the traditional calibration while starting to implement the time-domain calibrator on the more simple interferometer modes. In weeks five and six, we will continue working on the time-domain calibrator by moving on to more advanced interferometer modes. In weeks seven and eight, we hope to complete the time-domain calibrator for the Caltech 40m by integrating all the separate mode signals into a single calibration. In weeks nine and ten, I will complete my final report and presentation in addition to traveling to Livingston to see the aLIGO detectors.

5 Progress

Since at Caltech, I have been working to gain the necessary skills to write a front end time domain calibration system. I have gone through Simulink, Feedback Control Systems, and Signal Processing tutorials for MATLAB to understand the tools required for my project. Additionally, I have been working toward completely understanding the frequency domain calibration model for Initial LIGO so I can soon begin writing a calibration model myself using MATLAB and Simulink. I hope to spend most of the next month writing parts of code for the time domain calibrator and testing them thoroughly with the help of my mentors.

The most challenging part of this project is understanding and correctly modeling the LIGO control systems. My next immediate task is to understand signal whitening and aliasing and how those affect the component transfer functions of the open loop gain $G_L(f)$. I hope to have begun actual code on the time domain calibration by the end of this week.

Over the past month I have worked on fully understanding the aLIGO control system Simulink models made by Jeff Kissel and Rana Adhikari. During this time I have come to understand the model well, and have found some bugs within the models themselves. For the past week, I have been attempting to implement Equation (9) in a Simulink block subsystem within Adhikari's model to replicate strain in the frequency domain. However, inverting the sensing function C_L is
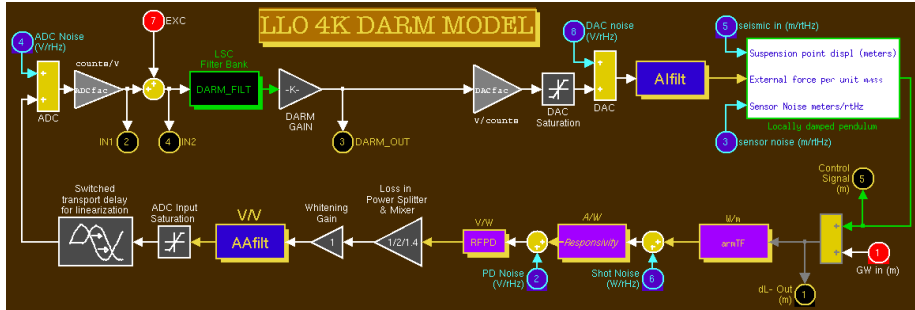
Figure 6: Control System Model created by Rana Adhikari. [6]

very difficult in Simulink due to instabilities: Simulink does not allow systems with more zeros than poles in their transfer functions to be implemented.

To combat this problem, we have introduced artificial poles at high frequency to create a stable system that Simulink accepts. However, even with this stable system, any input into the inverted sensing function will exponentially blow up to infinity.

As of this writing, the cause of this problem appears to be due to a time delay. In such a system, a time delay is equivalent mathematically to a frequency dependant phase shift. This phase shift appears to be causing some poles in the inverted sensing function to have positive real part components. Positive real components in a pole will result in an unstable system due to exponential growth, so it appears this signal time delay is the cause of the instability. Since the delay is very important to the overall control system, we have moved on to implementing a simplified version of the inverted sensing function as of this writing.

My goal for the project is to return to the 40m interferometer and begin an implementation of the time domain calibration control system there. First, I need to construct a matrix relating the real time changes in the parameters to the calibration line fluxuations. Then, if this matrix is invertable, we ought to be able to use the calibration lines in conjunction with the inverted matrix to track the parameter changes in real time and update our control system parameters in situ.

References

[1] LIGO Scientific Collaboration (Abadie, J. et al.) Nucl.Instrum.Meth. A624 (2010) 223-240 arXiv:1007.3973 [gr-qc]

[2] Siemens, X., et al., 2004. Making $h(t)$ for LIGO. Class. Quantum Grav. 21 (S1723)

[3] Abbott, B. P., et al., 2009. LIGO: The Laser Interferometer Gravitatational-Wave Observatory. Rep. Prog. Phys. 72 (076901).

[4] J. Kissel. *Calibrating and Improving the Sensitivity of the LIGO Detectors.* PhD thesis, Lousiana State University, 2010.

[5] R. Adhikari. *Sensitivity and Noise Analysis of 4 km Laser Interferometric Gravitational Wave Antennae.* PhD thesis, Massachusetts Institute of Technology, 2004.

[6] R. Adhikari. *LLO 4K DARM Model.* Simulink/MATLAB Model, California Institute of Technology, 2013.